JCB Article

Yeast homotypic vacuole fusion requires the Ccz1–Mon1 complex during the tethering/docking stage

Chao-Wen Wang,[1] Per E. Stromhaug,[1] Emily J. Kauffman,[2] Lois S. Weisman,[2] and Daniel J. Klionsky[1]

[1]Life Sciences Institute and the Department of Molecular, Cellular and Developmental Biology and Biological Chemistry, University of Michigan, Ann Arbor, MI 48109
[2]Department of Biochemistry, University of Iowa, Iowa City, Iowa 52242

The function of the yeast lysosome/vacuole is critically linked with the morphology of the organelle. Accordingly, highly regulated processes control vacuolar fission and fusion events. Analysis of homotypic vacuole fusion demonstrated that vacuoles from strains defective in the *CCZ1* and *MON1* genes could not fuse. Morphological evidence suggested that these mutant vacuoles could not proceed to the tethering/docking stage. Ccz1 and Mon1 form a stable protein complex that binds the vacuole membrane. In the absence of the Ccz1–Mon1 complex, the integrity of vacuole SNARE pairing and the unpaired SNARE class C Vps/HOPS complex interaction were both impaired. The Ccz1–Mon1 complex colocalized with other fusion components on the vacuole as part of the cis-SNARE complex, and the association of the Ccz1–Mon1 complex with the vacuole appeared to be regulated by the class C Vps/HOPS complex proteins. Accordingly, we propose that the Ccz1–Mon1 complex is critical for the Ypt7-dependent tethering/docking stage leading to the formation of a trans-SNARE complex and subsequent vacuole fusion.

Introduction

Membrane fusion must be tightly catalyzed and regulated to ensure correct compartmentalization in eukaryotic cells. Biochemical and molecular genetic studies have identified conserved families of proteins that catalyze donor/acceptor membrane recognition and fusion. These include the NSF protein, SNAPs, the SNAP receptor complex, and the rab GTPase and Sec1 families of proteins. Members of these latter two protein families have been suggested to act in concert with the SNARE proteins to provide the specificity and efficiency of membrane docking and fusion. In addition, many accessory factors involved in membrane fusion at specific locations within the cell have been identified, such as the Exocyst, TRAPP, the VFT complex, and the class C Vps (C-Vps)/HOPS (homotypic fusion and vacuole protein sorting) complex. These factors appear to assemble into protein complexes and facilitate the membrane docking/fusion stage by interacting with a rab family small GTPase.

In the budding yeast *Saccharomyces cerevisiae*, the analysis of homotypic vacuole fusion has expanded our understanding of membrane fusion events. A biochemical dissection of this process has identified four distinct stages (Fig. 1; for reviews see Wickner and Haas, 2000; Wickner, 2002). During the first step, priming, Sec18 (yeast NSF) utilizes ATP to drive the release of Sec17 (α-SNAP) from a cis-SNARE complex and the transfer of a novel chaperone, LMA1, from Sec18 to the t-SNARE Vam3. Priming also results in the disassembly of the cis-SNARE complex and release of the C-Vps/HOPS complex from the SNAREs. The primed vacuoles then come into contact in the tethering/docking steps. Docking begins with tethering, which requires the interaction of the C-Vps/HOPS complex with the rab GTPase Ypt7. Stable docking requires a membrane electrochemical potential, Rho GTPases, phosphoinositides, and trans-SNARE pairing. The precise events that occur during fusion are still an open question, however, the release of Ca^{2+} at the conclusion of docking causes calmodulin binding to the vacuole membrane and the interaction of V_0-V_0 domains of the vacuolar ATPase in trans. Protein phosphatase 1 activity and release of LMA1 and Vac8 are also involved at a very late stage of fusion. A recent report analyzed vertex membranes at the rim of the connected vacuoles where membrane fusion and fusion pore expansion occurs. Proteins needed for docking and fusion are not evenly distributed on the vacuole but accumulate at the vertices.

Address correspondence to Daniel J. Klionsky, University of Michigan, Life Sciences Institute, Ann Arbor, MI 48109-2216. Tel.: (734) 615-6556. Fax: (734) 647-0884. email: klionsky@umich.edu

Key words: class C Vps; HOPS; membrane fusion; Rab; SNAREs

Abbreviations used in this paper: AD, activation domain; ARS, ATP regeneration system; BD, binding domain; C-Vps, class C Vps; Cvt, cytoplasm-to-vacuole targeting; PA, protein A; SMD, synthetic minimal medium with dextrose.

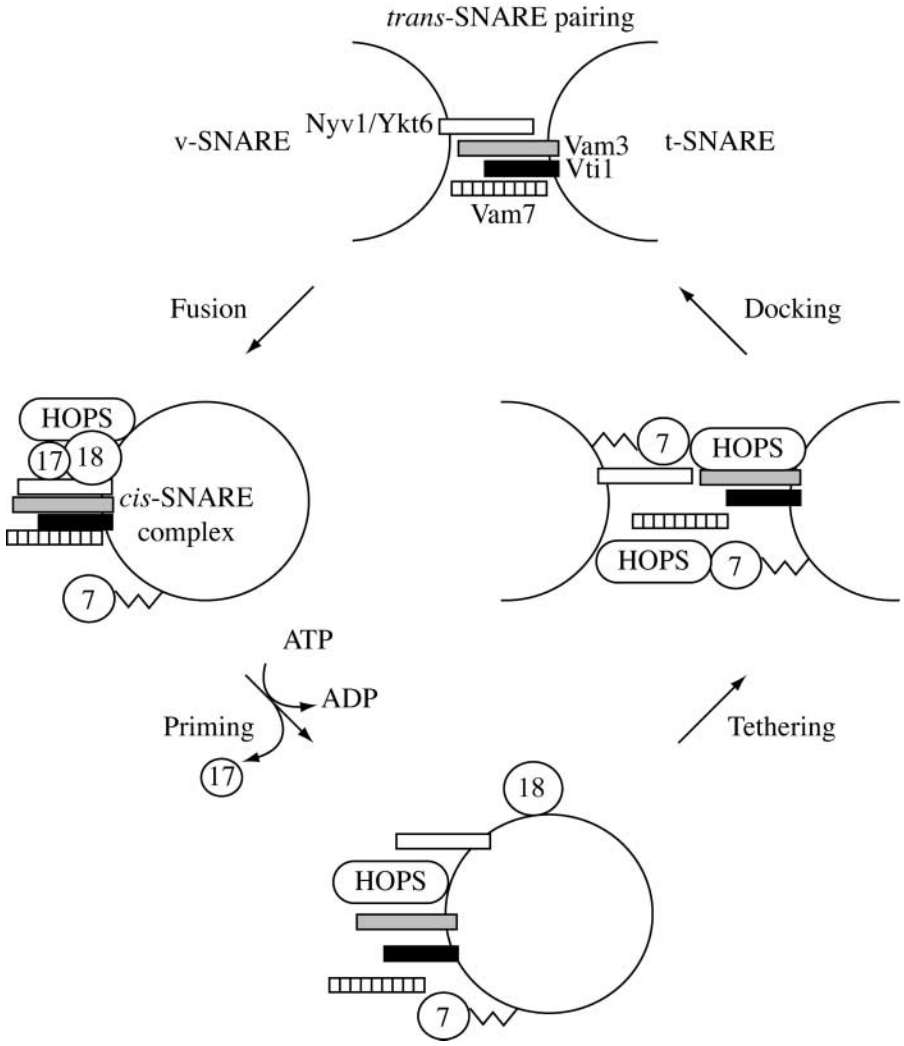

Figure 1. **Working model for yeast homotypic vacuole fusion.** The R SNAREs Nyv1 and Ykt6 (white), and the Q SNAREs Vam3 (light gray), Vti1 (black), and Vam7 (striped) are indicated. The numbered circles correspond to Ypt7, Sec17, and Sec18. The C-Vps/HOPS protein complex comprises Vps11/Pep5, Vps16, Vps18/Pep3, Vps33, Vps39/Vam6, and Vps41. See text for details. Modified from Wickner and Haas, 2000.

The cytoplasm-to-vacuole targeting (Cvt) pathway, a constitutive pathway that is similar to macroautophagy, is used to deliver the soluble hydrolase Ape1 to the vacuole (for review see Stromhaug and Klionsky, 2004). We have shown that strains lacking two proteins, Ccz1 and Mon1, exhibit highly fragmented vacuole phenotypes (Wang et al., 2002a). Both Mon1 and Ccz1 are required for protein delivery through the Cvt pathway and other vacuole trafficking processes including the CPY and ALP pathways and endocytosis (Wang et al., 2002a). Biochemical characterization indicates that Ccz1 and Mon1 are needed for the Cvt pathway during the fusion stage, and the two proteins appear to be assembled in a stable protein complex. To extend our analysis, we examined the mechanism of action of the Ccz1 and Mon1 proteins. We now present evidence that Ccz1 and Mon1 are also needed for yeast homotypic vacuole fusion. We found that the Ccz1–Mon1 complex binds to the vacuole membrane in a cooperative manner; neither protein is found at the vacuole in strains lacking the complementary component. Without the Ccz1–Mon1 complex, vacuole fusion was blocked at a stage before tethering/docking. Biochemical evidence indicated that the Ccz1–Mon1 complex is part of the vacuolar SNARE complex and is disassembled and released from the vacuole during ATP-dependent vacuole fusion. Moreover, the C-Vps/HOPS complex is involved in regulating the vacuole membrane association of the Ccz1–Mon1 complex. Therefore, our findings reveal a critical role for the Ccz1–Mon1 complex in maintaining proper vacuole morphology by regulating fusion at the tethering/docking stage.

Results

The Ccz1–Mon1 complex is required for homotypic vacuole fusion

Ccz1 and Mon1 are required for multiple trafficking pathways to the vacuole including the Cvt pathway (Wang et al., 2002a). In a *ccz1*Δ or *mon1*Δ mutant, the Cvt pathway is blocked because the fully formed Cvt vesicles fail to fuse with the vacuole; precursor Ape1 accumulates in a protease-protected state (Wang et al., 2002a). Accordingly, one of the speculations concerning the function of the Ccz1–Mon1 complex is that the two proteins might have a general role in vacuole fusion. To explore the function of the Ccz1–Mon1 complex in fusion of Cvt vesicles with the vacuole, we first determined whether the complex plays a role during homotypic vacuole fusion. An assay to measure yeast homotypic vacuole fusion has been developed by Wickner (2002). In

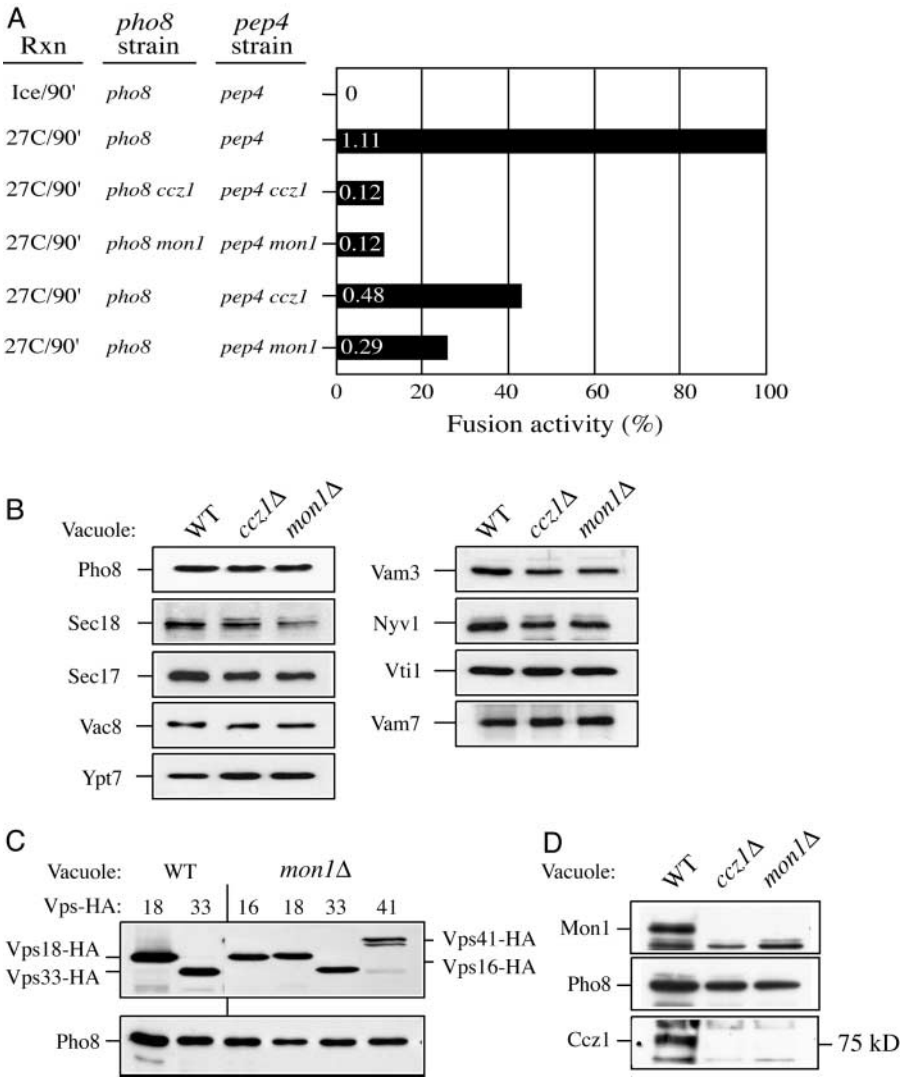

Figure 2. **Vacuoles from *ccz1*Δ and *mon1*Δ strains are defective in homotypic fusion.** (A) Vacuoles from strains DKY6281 (*pho8*Δ), BJ3505 (*pep4*Δ), CWY15 (*ccz1*Δ *pho8*Δ), CWY34 (BJ3505 *ccz1*Δ), CWY14 (*mon1*Δ *pho8*Δ), and CWY33 (BJ3505 *mon1*Δ) were analyzed for homotypic fusion as described in Materials and methods. The relevant genetic markers are indicated. Fusion activity is presented as percentage values normalized to the wild-type vacuole control, which was set at 100%. The corresponding alkaline phosphatase activities (expressed as units) are indicated within the bars. The background activity (0.15 units) from the sample kept on ice was subtracted from all other samples. (B) Proteins required for vacuole–vacuole fusion are targeted to the *ccz1*Δ and *mon1*Δ vacuoles. Vacuoles prepared from the BJ3505, BJ3505 *ccz1*Δ, and BJ3505 *mon1*Δ strains were TCA precipitated, and proteins were detected by Western blot as indicated. (C) C-Vps/HOPS proteins are bound to the *mon1*Δ vacuoles. Vacuoles prepared from the BJ3505 or BJ3505 *mon1*Δ background containing the indicated HA fusion forms of C-Vps components were TCA precipitated, and proteins were detected by Western blot against HA and Pho8 as a loading control. (D) Cooperative binding of Ccz1 and Mon1 to the vacuole. Vacuoles prepared from the BJ3505, BJ3505 *ccz1*Δ, and BJ3505 *mon1*Δ strains were TCA precipitated, and proteins were detected by Western blot against Pho8, Mon1, and Ccz1.

brief, vacuoles are prepared from a *pep4*Δ strain that supplies the inactive precursor form of alkaline phosphatase (Pho8), and from a *pho8*Δ strain that provides vacuolar proteinase A (Pep4) processing activity. If the two pools of vacuoles fuse in vitro, precursor Pho8 is activated. Vacuoles from wild-type and mutant strains were prepared as described in Materials and methods. Standard reactions were incubated at 27°C or on ice for 90 min. Pho8 activity from the fusion of wild-type vacuoles at 27°C was defined as 100%, and a control sample on ice was defined as 0%. Data from three independent experiments are summarized in Fig. 2 A. When both sets of vacuoles were from the *ccz1*Δ and *mon1*Δ strains, fusion activity decreased to 10% of wild-type vacuoles. The fusion activities were increased if *ccz1*Δ and *mon1*Δ vacuoles were incubated in the reaction with wild-type vacuoles, however, the fusion activity was still well below that when the vacuole pairs were both wild type. The fact that both mutant vacuoles are morphologically fragmented (Fig. 2; Wang et al., 2002a), coupled with the in vitro fusion defect, suggests that both the *ccz1*Δ and *mon1*Δ strains are defective in homotypic vacuole fusion.

Many of the general components required for vacuolar fusion have been identified (Wickner, 2002). To determine if the homotypic vacuole fusion defects of the *ccz1*Δ and *mon1*Δ strains were due to the absence of molecules known to be required for fusion, we TCA precipitated proteins from purified vacuoles of wild-type and mutant strains and examined protein levels by Western blot. We found that the peripherally associated proteins including Sec18 (NSF), Sec17 (α-SNAP), Vac8, and Ypt7 (Rab) were on both wild-type and mutant vacuoles (Fig. 2 B). Vacuolar SNARE proteins including Vam3, Nyv1, Vti1, and Vam7 are also present on the vacuoles in the *ccz1*Δ and *mon1*Δ strains at levels similar to those seen on the wild-type vacuoles (Fig. 2 B). Similarly, we found that the C-Vps components were also present on the vacuoles of the mutant strains (Fig. 2 C; unpublished data). Accordingly, we concluded that the fusion defect for the two mutants was not due to loss of these previously identified components. However, as shown in Fig. 2 D, we found that the *ccz1*Δ strain failed to recruit Mon1 on the purified vacuoles, and vice versa. These data, along with the analysis of the role of Ccz1 and Mon1 in the Cvt pathway (Wang et al., 2002a) demonstrate that these two proteins form a stable complex.

One strategy to demonstrate that a protein directly participates in homotypic vacuole fusion is to inhibit the in

vitro fusion reaction by the addition of affinity-purified antiserum against the protein of interest. However, the success of this approach depends on the affinity of the particular antibody. We found that affinity-purified antiserum against Ccz1 or Mon1 was not able to inhibit the reaction (unpublished data). Accordingly, we adopted an alternative approach. We generated strains with protein A (PA) fusion to Ccz1 and Mon1 to take advantage of the specific affinity between PA and the F_c region of IgG. Fig. 3 A shows a Western blot against vacuole proteins from two fused partner strains, the *pho8*Δ (DKY6281, DK) and *pep4*Δ (BJ3505, BJ) strains, containing integrated copies of Ccz1-PA and Mon1-PA. The COOH-terminal PA fusion forms of Ccz1 and Mon1 are stable proteins, are both associated with the vacuole, and are maintained at similar levels to their corresponding wild-type proteins. PA tagging did not affect Ccz1 and Mon1 function because all of the tagged strains exhibited normal vacuole morphology in vivo (unpublished data). Furthermore, the purified vacuoles showed fusion activities that were comparable to wild-type vacuoles (Fig. 3 B). As a control, we treated the vacuoles with an antiserum against a protein that is not localized to the vacuole and does not play a role in fusion. We found that treating with this antiserum did not affect wild-type vacuole fusion activity in vitro. However, the fusion activity decreased to 80% when Ccz1-PA was present on both of the fusion partners. Furthermore, when both vacuole partners harboring Mon1-PA were tested, the fusion activity was reduced to 26%. This reduction is similar to inhibition of vacuole fusion with affinity-purified antiserum to Sec18 (Kato and Wickner, 2003). Fusion activities in the presence of antiserum were substantially decreased if either one of the vacuoles contained Mon1-PA. These data suggest that at least Mon1 has a direct role in homotypic vacuole fusion. Vacuoles with Ccz1-PA treated with antibody displayed a smaller defect in fusion (20%). This reduction in fusion activity may be indirect and reflect the requirement for Ccz1 in vacuolar recruitment of Mon1. Alternatively, the differ-

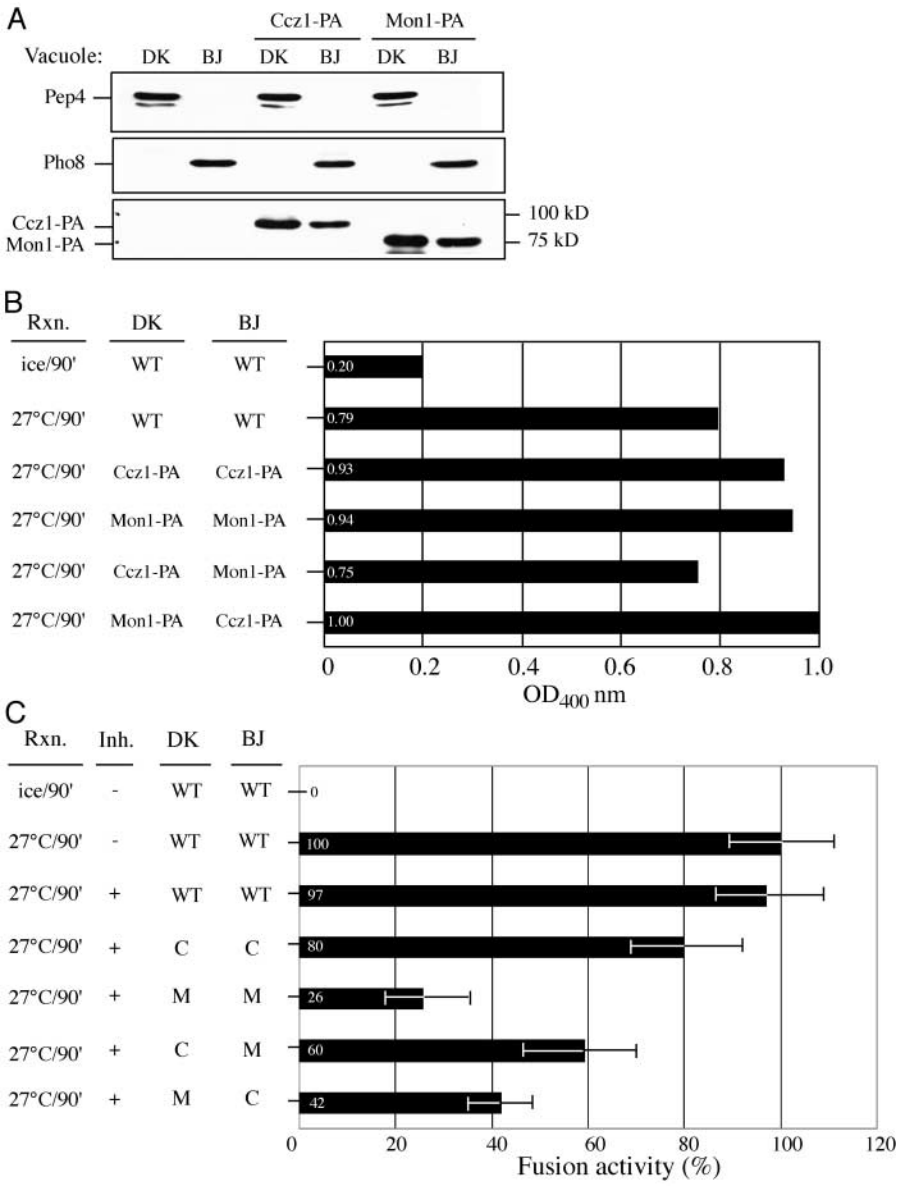

Figure 3. **An inhibition assay reveals a direct requirement of Mon1 during fusion.** (A) Vacuolar protein levels of Ccz1-PA and Mon1-PA. Vacuoles purified from two parental strains, DKY6281 (*pho8*Δ, DK) and BJ3505 (*pep4*Δ, BJ), were TCA precipitated and assayed by Western blot against Pho8 and Pep4. The relevant genetic markers are indicated. The PA fusion forms of Ccz1 and Mon1 were detected by Western blot against PA. (B) Vacuoles containing Ccz1-PA and Mon1-PA fuse in vitro. Vacuoles were analyzed for homotypic fusion as described in Materials and methods. The relevant genetic markers are indicated. Each experiment was assayed and averaged from three independent fusion reactions. Fusion activities were shown as measured by OD_{400} nm. (C) Inhibition assay. Vacuoles were analyzed for homotypic fusion. Antiserum was added in the fusion reaction as described in Materials and methods. Each experiment was assayed and averaged from six independent fusion reactions. All fusion activities were indicated as percentage compared with their corresponding vacuole fusion activity when the antiserum was not added as shown in B.

ence in inhibition may reflect steric differences resulting from F_c binding to the particular PA construct.

Ccz1 and Mon1 are required for the coordinated priming and tethering/docking stage of fusion

It has been proposed that three distinct events are essential for the homotypic fusion pathway: priming, tethering/docking, and fusion (Wickner and Haas, 2000). To gain a better understanding of the stage where the *ccz1*Δ and *mon1*Δ vacuoles were blocked in fusion, we performed a microscopy assay to determine if the *ccz1*Δ and *mon1*Δ vacuoles are able to dock (Wang et al., 2001b). Vacuoles were purified and incubated in standard reactions with (1) the omission of ATP, to prevent priming and the subsequent docking and fusion steps; (2) the addition of the calcium chelator BAPTA that inhibits a post-docking fusion step; (3) the complete reaction at 27°C for 90 min where wild-type vacuoles fuse; and (4) the incubation on ice for 90 min to prevent fusion. Incubation on ice at the start of the reaction prevents initiation of the fusion reaction, and vacuoles were dispersed throughout the field (Fig. 4 A). Similarly, both wild-type and mutant vacuoles were unable to dock and were randomly dispersed when priming was blocked by the deprivation of ATP. Wild-type vacuoles incubated with ATP and BAPTA were able to prime and dock but could not fuse. In this case, the vacuoles appeared as clumps. In the absence of BAPTA, wild-type vacuoles fused and were several times larger than the docked vacuoles. In contrast, *ccz1*Δ, *mon1*Δ, and *ypt7*Δ vacuoles remained dispersed in the presence of ATP and BAPTA and did not show an increase in size in the presence of ATP alone (Fig. 4 A). Quantification of these results from multiple fields is summarized in Table I. We found that *ccz1*Δ and *mon1*Δ vacuoles exhibited high percentages of individual vacuoles under all conditions, similar to the results observed with the *ypt7*Δ vacuoles. Moreover, mutant vacuoles were distinct from wild-type vacuoles, which give higher "contact per vacuole" scores following BAPTA treatment or when fusion was performed at 27°C for 90 min. These data

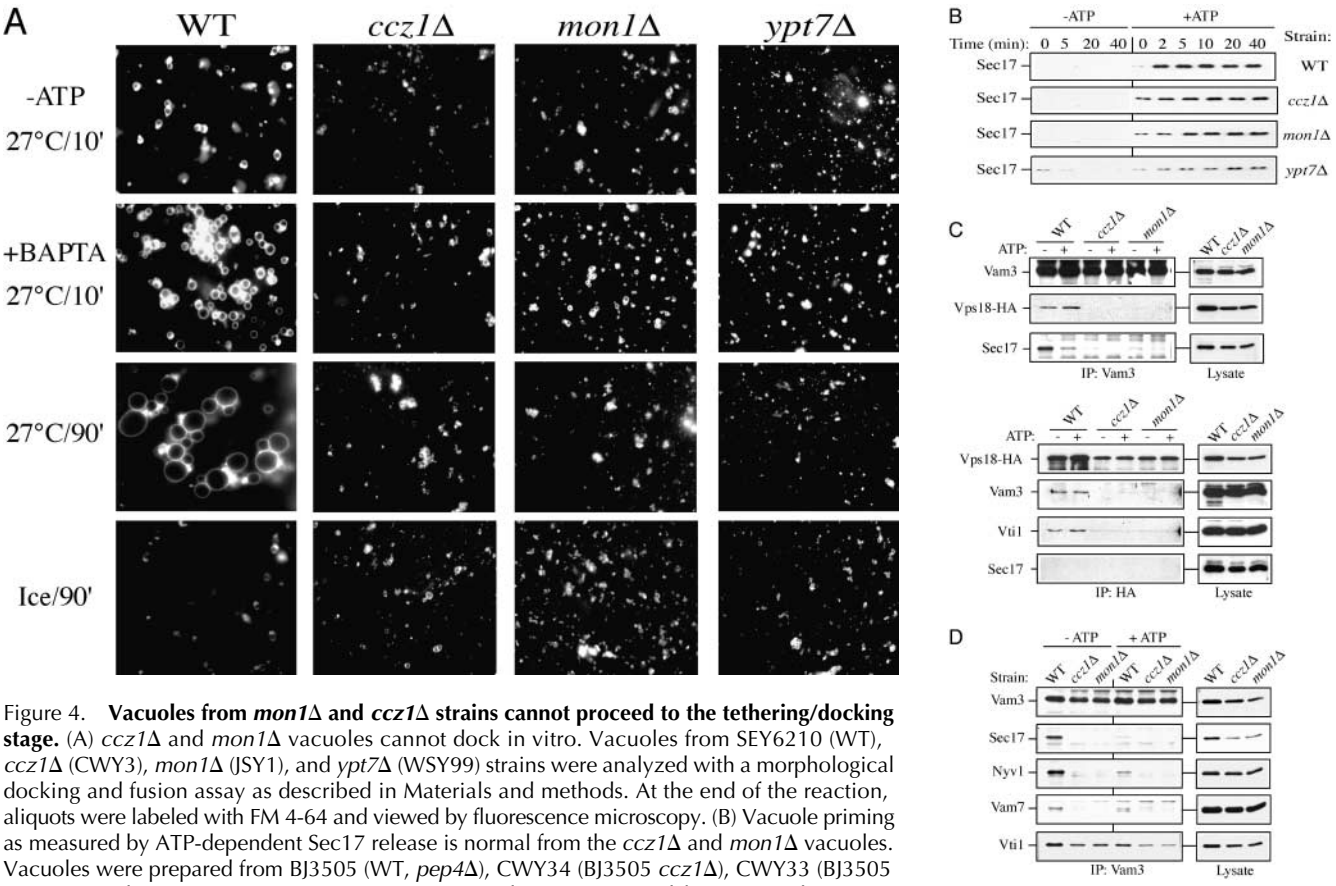

Figure 4. **Vacuoles from *mon1*Δ and *ccz1*Δ strains cannot proceed to the tethering/docking stage.** (A) *ccz1*Δ and *mon1*Δ vacuoles cannot dock in vitro. Vacuoles from SEY6210 (WT), *ccz1*Δ (CWY3), *mon1*Δ (JSY1), and *ypt7*Δ (WSY99) strains were analyzed with a morphological docking and fusion assay as described in Materials and methods. At the end of the reaction, aliquots were labeled with FM 4-64 and viewed by fluorescence microscopy. (B) Vacuole priming as measured by ATP-dependent Sec17 release is normal from the *ccz1*Δ and *mon1*Δ vacuoles. Vacuoles were prepared from BJ3505 (WT, *pep4*Δ), CWY34 (BJ3505 *ccz1*Δ), CWY33 (BJ3505 *mon1*Δ), and CWY23 (*ypt7*Δ *pep4*Δ) strains. Vacuoles were assayed for Sec17 release as described in Materials and methods. Supernatant fractions were TCA precipitated and examined by Western blot analysis for the presence of Sec17. (C) Assay for SNARE and C-Vps/HOPS interaction. Vacuoles from strains CWY42 (WT, BJ3505 *VPS18-HA*), CWY57 (BJ3505 *ccz1*Δ *VPS18-HA*), and CWY47 (BJ3505 *mon1*Δ *VPS18-HA*) were mixed in 750-μl vacuole fusion reactions with the addition of apyrase (−ATP) or ARS (+ATP). Reactions were incubated at 27°C for 15 min. Vacuoles were reisolated by centrifugation at 10,000 *g* for 5 min and then resuspended in HEPES immunoprecipitation buffer. A 10-μl aliquot of the lysates was used as a loading control. Solubilzed vacuoles were immunoprecipitated with anti-Vam3 (upper panel) or anti-HA (lower panel) antibody, and the presence of Vps18-HA, Vam3, Vti1, and Sec17 was assessed by Western blot. (D) Assay for total SNARE pairs present on isolated vacuoles and the ability of the pairs to be disrupted. Vacuoles were mixed in 750-μl vacuole fusion reactions and treated as described in C. Vacuoles from BJ3505 (WT), CWY34 (BJ3505 *ccz1*Δ), and CWY33 (BJ3505 *mon1*Δ) strains were immunoprecipitated (IP) with anti-Vam3 antibody, and the presence of Vam3, Sec17, Nyv1, Vam7, and Vti1 was assessed by Western blot.

Table I. The *ccz1*Δ and *mon1*Δ mutants are defective in docking

Reaction conditions	Strain	Number of vacuoles in cluster (%)				Total vacuoles	Contacts/vacuole
		○	○○	○○○	≥○○○		
	WT	79.3	5.8	4.7	10.2	429	1.7
−ATP	*ccz1*Δ	89.2	3	3.3	4.5	2152	1.3
	*mon1*Δ	90	4	2.6	3.4	1497	1.6
	*ypt7*Δ	90.8	3.4	2.6	3.2	1338	1.2
	WT	44	4.3	5.2	46.5	591	5.1
+BAPTA	*ccz1*Δ	89.1	2.7	3.3	4.9	1043	1.7
27°C/10 min	*mon1*Δ	89.7	2.2	2.2	5.9	1832	1.3
	*ypt7*Δ	90.4	1.2	1.9	6.5	1206	1.3
	WT	39.2	8	3.8	49	554	3.4
27°C/90 min	*ccz1*Δ	88.4	2	1.6	8	1334	1.2
	*mon1*Δ	87	2.5	3	7.5	956	1.1
	*ypt7*Δ	85.1	2.7	1.7	10.5	1112	1.6
	WT	93.2	2.9	1.9	2	752	1.1
Ice/90 min	*ccz1*Δ	96	1.4	1.2	1.4	1558	1.1
	*mon1*Δ	89.8	2.4	2.2	5.6	1353	1.3
	*ypt7*Δ	87.4	2.8	2	7.8	1446	1.4

suggest that the inability of vacuoles from the *ccz1*Δ and *mon1*Δ strains to fuse (Fig. 2 A) was due to a defect before tethering/docking.

We extended our analysis to further investigate whether it is priming or tethering/docking that is impaired in these mutants. During priming, Sec18 utilizes ATP to drive the release of Sec17 from the vacuole membrane and disassemble cis-SNARE complexes. Accordingly, we monitored Sec17 release from the wild-type, *ccz1*Δ, *mon1*Δ, and *ypt7*Δ vacuoles as described in Materials and methods. Without the addition of ATP, Sec17 remained attached to the vacuole membrane and was not detected in the supernatant fraction (Fig. 4 B). The addition of ATP in the reaction mixture caused Sec17 to be quickly released from the wild-type vacuoles where it could be recovered in the supernatant fractions. Similar results were also observed with vacuoles from the *ccz1*Δ, *mon1*Δ, and *ypt7*Δ strains (Fig. 4 B), suggesting that priming, as monitored by Sec18-dependent Sec17 release, was functional with these mutant vacuoles.

According to the working model for homotypic vacuole fusion, the major event after Sec18-dependent priming is the disassembly of the cis-SNARE complex that allows the formation of SNARE pairs in trans through the function of a Rab protein (Wickner and Haas, 2000). Ypt7 interacts with the C-Vps/HOPS complex comprised of Vps11, Vps16, Vps18, Vps33, Vps39, and Vps41 and is required for the vacuoles to dock (Sato et al., 2000; Wurmser et al., 2000). A critical event during the docking stage is the interaction between the C-Vps complex and the unassembled t-SNARE Vam3 to achieve trans-SNARE pairing. To monitor this event, we performed a Vam3 coimmunoprecipitation using a strain with HA-tagged Vps18 to see if the unassembled Vam3 on the *mon1*Δ and *ccz1*Δ vacuoles was able to interact with the C-Vps/HOPS complex. Vps18-HA is present on the purified vacuoles of the wild-type, *ccz1*Δ, and *mon1*Δ strains (Fig. 4 C). Vam3 on wild-type vacuoles coprecipitated Vps18-HA and Sec17 in the presence and absence of ATP (Fig. 4 C). The Vps18-HA levels appeared to increase slightly after 15 min in the presence of ATP, whereas Sec17 levels were reduced following ATP-dependent priming. In contrast, Vam3 did not coprecipitate Vps18-HA in either the *mon1*Δ or *ccz1*Δ strain. In addition, we performed the same reaction conditions using anti-HA antibody for the immunoprecipitation to pull-down proteins that are in a complex with Vps18-HA. We found that the SNARE proteins including Vam3 and Vti1 are present in the immune complex with Vps18-HA on the wild-type vacuoles, whereas Sec17, Nyv1, and Vam7 were absent from the same immune complex (Fig. 4 C; data not shown). These data support the previous findings that the C-Vps/HOPS proteins interact with the "unpaired" Vam3 that should be observed only when Sec17 is released from the cis-SNARE complex. With both *ccz1*Δ and *mon1*Δ vacuoles, we did not detect any Vam3 or Vti1 in the immune complex with Vps18-HA, although these proteins were present at levels similar to those of wild-type vacuoles. Therefore, we conclude that the tethering/docking stage was completely blocked when the Ccz1–Mon1 complex was omitted. Because the proposed role of the C-Vps/HOPS complex is to mediate SNARE pairing, we next checked whether SNARE pairs formed on these two mutant vacuoles. To investigate SNARE pairing, we set up two identical reactions in the absence or presence of ATP for 15 min followed by immunoprecipitation using anti-Vam3 antiserum. In the absence of ATP, cis-SNARE complexes were identified from the wild-type vacuole based on the coprecipitation of Sec17, Nyv1, Vam7, and Vti1 with Vam3 (Fig. 4 D). The cis-SNARE complex is disassembled in the presence of ATP and reduced levels of these proteins were coprecipitated with Vam3. We could not detect Nyv1 and Vam7 being pulled down by anti-Vam3

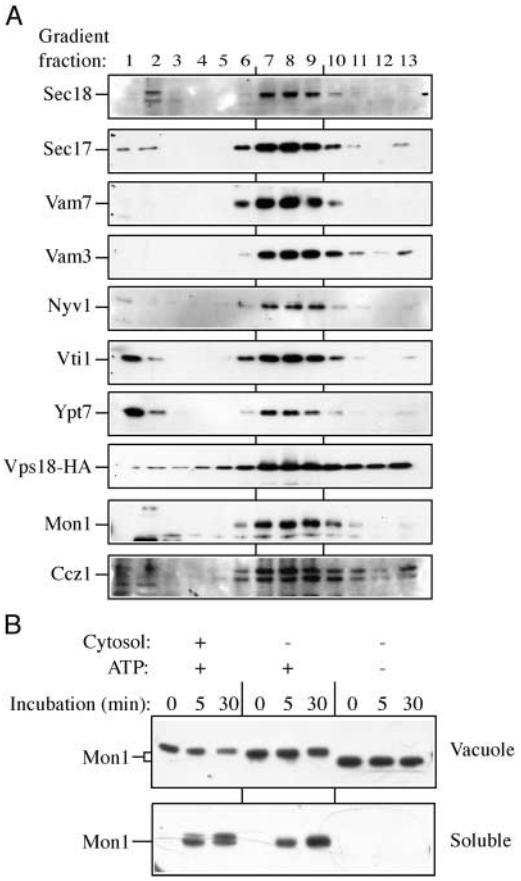

Figure 5. **Ccz1 and Mon1 constitute part of the vacuolar cis-SNARE complex.** (A) Vacuolar Ccz1 and Mon1 colocalize with proteins required for fusion. Vacuoles were prepared from strain CWY42 and were solubilzed as described in Materials and methods. Solubilized proteins were then resolved by a 10–60% sucrose gradient as described in Materials and methods, and proteins were assayed by Western blot. (B) Mon1 release from the vacuole requires ATP. Vacuoles were prepared from the BJ3505 strain. Vacuoles were assayed for the release of Mon1 as described in Materials and methods. The vacuole and its relevant supernatant (soluble) fractions were TCA precipitated separately and subjected to Western blot against Mon1. Reactions with ATP include an ATP regeneration system.

from the *ccz1*Δ and *mon1*Δ vacuoles even though all of these proteins were present (Figs. 2 B and 4 D). Furthermore, we found that Sec17 was also absent from the Vam3 complex even though Sec18-dependent Sec17 release was functional on the *ccz1*Δ and *mon1*Δ vacuoles (Fig. 4 B). We found that Vti1 was the only SNARE that was in a complex with Vam3 on the *ccz1*Δ and *mon1*Δ vacuoles, and the disassembly of this complex appeared to be similar to that on the wild-type vacuoles. We conclude that the absence of Ccz1 or Mon1 affects vacuolar SNARE pair association. Together, we propose that the Ccz1–Mon1 complex is required for vacuole fusion by regulating the coordinated priming and tethering/docking stages.

The Ccz1–Mon1complex on the vacuole is assembled as part of the cis-SNARE complex

Many proteins known to be needed for homotypic vacuole fusion are found on the vacuole as a cis-SNARE complex, which represents the end product of a previous round of fusion (Wickner and Haas, 2000; Wickner, 2002). We have shown that both Ccz1 and Mon1 are localized on the purified vacuoles and they appear to tightly associate with each other (Fig. 2 D). Next, we examined if Ccz1 and Mon1 are assembled inside the vacuolar cis-SNARE complex. We performed a sucrose density gradient analysis by loading detergent-solublized vacuoles on the top of the gradient. We found that identified fusion components such as Sec18, Sec17, and SNAREs copeaked in fractions 7 to 9 (Fig. 5 A). The majority of Ypt7 appeared to float in the top fraction of this gradient; however, a minor peak of Ypt7 was also present in fractions 7 to 9. Accordingly, we refer to this peak as the previously identified cis-SNARE complex. Furthermore, we found that the C-Vps protein Vps18-HA colocalized with Ccz1 and Mon1 at this cis-SNARE complex peak (Fig. 5 A). The finding that these proteins were assembled into the end product of fusion, the cis-SNARE complex, supports the hypothesis that the Ccz1–Mon1 complex directly participates in fusion.

Vacuoles fuse in vitro in the presence of ATP. The addition of ATP leads to dissociation of the cis-SNARE complex allowing a rearrangement of fusion components in trans (Wickner and Haas, 2000). Accordingly, several proteins, including Sec17, release from the cis-SNARE complex on the vacuole membrane in a regulated process to initiate another cycle of fusion (Mayer et al., 1996). To see whether Mon1 undergoes a similar type of regulated release, we checked Mon1 behavior during the in vitro vacuole fusion assay (Fig. 5 B). Vacuoles were incubated in fusion reactions in the presence or absence of cytosol and/or ATP. Reactions were incubated at 27°C and were centrifuged to recover vacuole and supernatant fractions after 0, 5, and 30 min of incubation. We found that Mon1 remained attached tightly with the vacuole in the absence of ATP. In contrast, in the presence of ATP, some of the Mon1 was released from the vacuole and appeared in the supernatant fraction (Fig. 5 B). The molecular mass of vacuolar Mon1 appeared to increase in vitro when ATP was present. This size shift may be part of the regulation of Mon1; however, we could not detect the higher molecular weight form of Mon1 in vivo. Overall, our results suggest that the Ccz1–Mon1 complex dissociates from the SNARE complex and detaches from the vacuole membrane during fusion. Ccz1-GFP is recruited to the vacuole membrane immediately after osmotic induction of vacuole fusion in vivo (Wang et al., 2002a). Thus, the Ccz1–Mon1 complex is regulated during fusion in part by changes in its association with the vacuole membrane.

Regulation of the Ccz1–Mon1 complex through the C-Vps/HOPS complex

The interaction between Vps18-HA and unpaired Vam3 was impaired when Ccz1 or Mon1 was not present on the vacuole (Fig. 4 C). Ypt7 coprecipitates with Ccz1-HA, and Ypt7 overexpression rescues the *ccz1*Δ vacuole fragmentation phenotype (Kucharczyk et al., 2000, 2001). Therefore, we tested if the Ccz1–Mon1 complex participates in the Ypt7-dependent tethering/docking stage through its interaction with the C-Vps/HOPS complex. A report by Wang et al. has shown that SNAREs, Ypt7, and the C-Vps/HOPS

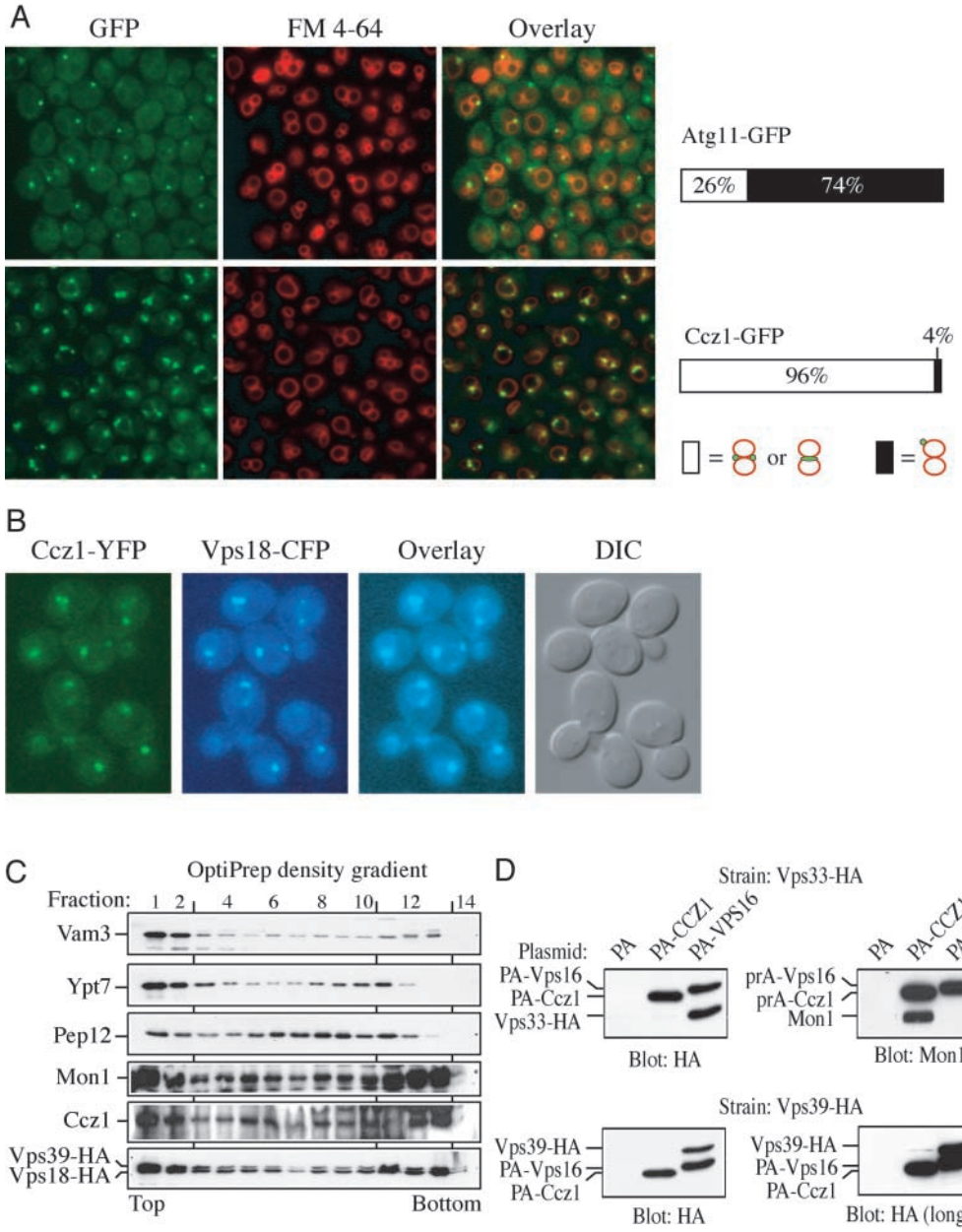

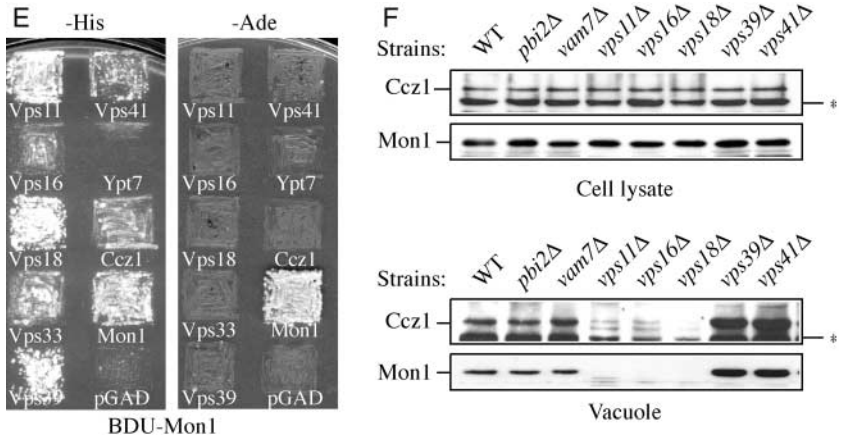

Figure 6. **The Ccz1–Mon1 complex is regulated by the C-Vps complex.** (A) Ccz1-GFP is enriched at vacuole–vacuole junctions. Strains PSY101 and PSY46 with integrated Atg11-GFP and Ccz1-GFP, respectively, were grown to mid log phase followed by FM 4-64 staining and fluorescent microscopy. 250 random "docked" vacuoles from several fields were scored, and the percentage of the fusion proteins that localize to (white), or do not localize to (black), the vacuole–vacuole junctions were tabulated. Note that only docked vacuoles (i.e., not individual vacuoles) were included in the calculations. (B and C) Colocalization of the Ccz1–Mon1 complex with the C-Vps/HOPS complex. (B) Colocalization of Ccz1-YFP and Vps18-CFP in vivo. Strain PSY43 with Ccz1-YFP and Vps18-CFP integrated at the chromosomal loci was grown to mid-log phase in SMD and examined by fluorescence microscopy. (C) Strain CWY173 (Vps39-HA Vps18-HA) was grown in YPD to mid-log phase and examined by density gradient centrifugation as described in Materials and methods. Fractions were examined by immunoblot against Vam3, Ypt7, Pep12, Ccz1, Mon1, and HA. (D) The C-Vps complex and the Ccz1–Mon1 complex are distinct protein

complex were enriched at vacuole–vacuole junctions (Wang et al., 2002b). We have previously published that Ccz1-GFP and Mon1-GFP localize to punctate structures on the vacuole membrane similar to C-Vps/HOPS complex proteins (Wang et al., 2002a). Accordingly, we decided to test whether the Ccz1-GFP signal was enriched at the vacuole–vacuole junctions. We used Atg11-GFP as a control. Atg11 is a protein required for the Cvt pathway and it has been shown to localize at a structure tightly associated with the vacuole (Kim et al., 2001), yet has no known role in homotypic vacuole fusion. We stained cells with the dye FM 4-64 to allow a clear observation of vacuole morphology. From multiple fields we counted 250 "docked" vacuoles and quantified the spatial localization of GFP as shown in Fig. 6 A. We found that 96% of the Ccz1-GFP signal was associated with the docked vacuole, whereas Atg11-GFP only displayed 26% association. Therefore, we concluded that the Ccz1-GFP signals were enriched at the vacuole–vacuole junctions reminiscent of the results seen with the HOPS proteins. To see if the Ccz1–Mon1 complex colocalizes with the C-Vps/HOPS complex, we generated a strain expressing both Ccz1-YFP and Vps18-CFP under their endogenous promoters. The Vps18-CFP signal was detected on the vacuole membrane as well as on punctate dots adjacent to the vacuoles. The dot structures colocalized with the Ccz1-YFP signal (Fig. 6 B). Using an OptiPrep™ gradient as described in Materials and methods, we tested whether Ccz1 and Mon1 colocalized with the C-Vps/HOPS complex proteins. Consistent with the Vps18-CFP localization in vivo, we detected a peak of Vps18-HA and Vps39-HA in the top few fractions that colocalized with most of the Vam3 and Ypt7, indicating vacuolar localization (Fig. 6 C). In addition to the top vacuole peak, the majority of the Vps18-HA and Vps39-HA (as well as all other C-Vps/HOPS members; data not shown) cofractionated with Ccz1 and Mon1 to a dense part of the gradient, suggesting that they colocalize to a higher density compartment. Together, the fluorescence and fractionation data suggest that the Ccz1–Mon1 complex colocalizes with a portion of the HOPS complex that is located in part at vacuole–vacuole junctions.

To further study the relationship between the Ccz1–Mon1 complex and the C-Vps/HOPS complex, we fused PA to the NH_2 terminus of Ccz1 and expressed this construct under the control of a copper inducible *CUP1* promoter (pCu-PA-CCZ1). The fusion protein complements the prApe1 sorting defect in the *ccz1*Δ strain (data not shown). We performed PA affinity chromatography using strains that had HA tags integrated at the chromosomal loci of the C-Vps/HOPS genes. These strains were transformed with plamids expressing PA alone, PA-Ccz1, or PA-Vps16. We recovered the PA immune complex using IgG sepharose as described in Materials and methods. All of the HA-tagged C-Vps/HOPS proteins including Vps33-HA and Vps39-HA were affinity isolated by PA-Vps16, but not PA-Ccz1 (Fig. 6 D; unpublished data). In contrast, Mon1 was only recovered by PA-Ccz1, but not PA-Vps16. When the anti-HA Western blots were exposed for a longer time, weak C-Vps/HOPS-HA signals could be seen with the PA-Ccz1 affinity isolation (Fig. 6 D; unpublished data). No proteins were recovered in the immune complex with PA alone, suggesting that binding was specific to the respective fusion proteins. Furthermore, purified vacuoles containing Vps18-PA affinity isolated low but significant levels of Mon1, suggesting that the C-Vps/HOPS complex and the Ccz1–Mon1 complex transiently or weakly interact (unpublished data). Similarly, using BDU-Mon1 as the bait, we found that Mon1 showed weak but positive yeast two-hybrid interactions with activation domain (AD) forms of C-Vps/HOPS components, especially Vps11, Vps18, and Vps39 (Fig. 6 E). Mon1 also interacted with Ccz1 and with itself by this two-hybrid assay on −His plates. In contrast, these interactions were not detectable under stronger selection (−Ade plate) except for the Mon1 self-interaction. Together, these data suggest that the Ccz1–Mon1 complex and the HOPS complex are not further assembled into a higher order complex although they appear to be colocalized at the same membrane compartments; instead they might interact transiently under steady-state conditions.

We have shown that Ccz1 and Mon1 are found on the vacuole together. To see how this binding is regulated, we looked at several vacuole fusion deficient mutants, including the individual C-Vps/HOPS null strains (Fig. 6 F). We found that the absence of C-Vps/HOPS components did not affect the level of Mon1 or Ccz1 under steady-state conditions. We then examined purified vacuoles from these strains. Although *pbi2*Δ and *vam7*Δ vacuoles, which lack components needed for fusion, accumulated wild-type levels of Ccz1 and Mon1, the vacuoles from the C-Vps/HOPS mutants exhibited two distinct profiles in terms of Mon1 and Ccz1 binding (Fig. 6 F, vacuole). Vacuoles from the *vps11*Δ, *vps16*Δ, and *vps18*Δ strains were almost completely devoid of Mon1 and Ccz1. In contrast, vacuoles from the *vps39*Δ and *vps41*Δ strains accumulated at least three times more Mon1 and Ccz1 than did wild-type vacuoles. These results indicated that the C-Vps/HOPS complex regulates the association of the Ccz1–Mon1 complex with the vacuole. Apparently one subcomplex of C-Vps/HOPS is required for stabilizing vacuolar Ccz1–Mon1, whereas the other subcomplex is involved in down-regulation of this

complexes. Strains PSY32 (Vps33-HA) and PSY33 (Vps39-HA) were transformed with plasmids expressing PA, PA-Ccz1, or PA-Vps16. Cells were grown in SMD followed by osmotic lysis. Lysates were incubated with IgG sepharose as described in Materials and methods. Bound proteins were detected by Western blot against HA or Mon1. (E) Mon1 exhibits a weak two-hybrid interaction with the C-Vps complex. The PJ69-4A strain was cotransformed with pBD-MON1 and pAD fusions with components as indicated. Cells were patched on plates without uracil, leucine, and histidine (−His) as a weak selection or without uracil, leucine, and adenine (−Ade) as a strong selection. (F) Binding of the Ccz1–Mon1 complex to the vacuole is regulated by the C-Vps complex. (Upper panel) Strains with the indicated genetic backgrounds were grown in YPD to mid-log phase (A_{600} = 1.0). Total cell lysates were prepared and assayed by Western blot against Ccz1 and Mon1. (Lower panel) Vacuoles were prepared from the corresponding strain backgrounds. Identical amounts of vacuole proteins were TCA precipitated and assayed by Western blot against Ccz1 and Mon1. The asterisks mark a nonspecific cross-reacting band.

complex from the vacuole. Furthermore, this result also supports our finding that one of the functions of the Ccz1–Mon1 complex is mediated by its interaction with Ypt7 and the C-Vps/HOPS complex and that these proteins are required for vacuole fusion at the tethering/docking stage.

Discussion

Ccz1 and Mon1 are required for homotypic vacuole fusion

Ccz1 and Mon1 are required for multiple vacuole delivery pathways including the autophagy/Cvt pathways, the Mvb and Vps pathways, and endocytosis (Wang et al., 2002a). Although these proteins had not been previously implicated in homotypic vacuole fusion, the defects in multiple vacuole delivery pathways suggested that Mon1 and Ccz1 might act at the general stage of fusion with the vacuole membrane. To elucidate the function of Mon1 and Ccz1, we characterized the role of these proteins in yeast homotypic vacuole fusion. Many of the components required for the different steps of priming, docking, and fusion have been identified through the in vitro fusion assay developed by Wickner and colleagues (Wickner and Haas, 2000; Wickner, 2002). We found that the *mon1*Δ and *ccz1*Δ strains were defective in homotypic vacuole fusion (Fig. 2 A). Fusion activity was approximately doubled if the reaction was performed with one set of vacuoles from either a *MON1* or *CCZ1* strain. The fusion activity, however, remained very low when one set of vacuoles was from the *ccz1*Δ strain and the other from *mon1*Δ cells (unpublished data). Thus, either Ccz1 and Mon1 are required on both membranes, or both proteins are required to be present on the same membrane. The absence of Ccz1 or Mon1 prevents the stable association of the remaining protein on the vacuole membrane (Fig. 2 D), making it difficult to assess a specific role for either individual protein. These proteins themselves are stable in the absence of the other protein (unpublished data). The *ccz1*Δ and *mon1*Δ vacuoles contained essentially normal levels of at least some of the identified fusion machinery components (Fig. 2, B and C). Thus, the fusion defect in these strains does not appear to be due to the absence of these essential components from the vacuole membrane. An inhibition assay revealed that antibody interference with Mon1 function resulted in a severe fusion defect (Fig. 3). In contrast, a relatively minor defect was observed with inhibition of Ccz1. This result suggests that the main function of Ccz1 is to recruit Mon1 to the vacuole membrane. Alternatively, Ccz1 may be required to further stabilize Mon1 during fusion. The observation that Ccz1 and Mon1 reside in the vacuolar cis-SNARE complex and undergo an ATP-dependent release from this complex during fusion (Fig. 5) strongly supports the hypothesis that Ccz1 and Mon1 participate in a regulated step of the fusion pathway.

Ccz1 and Mon1 are required for C-Vps/HOPS to bind a Vam3-Vti1 complex

Various models have been proposed to explain the function of the different proteins that are required for the fusion process. According to Rothman's tetrameric vacuole SNARE model, four helices, three "Q"-SNAREs, and one "R"-SNARE are required to form the functional trans-SNARE complex (McNew et al., 2000). However, it was recently proposed that a pentameric SNARE complex is required for yeast homotypic vacuole fusion (Ungermann et al., 1999). The cis-SNARE complex that results from fusion is thought to be thermodynamically stable (Fasshauer et al., 1997) and must be dissociated in an energy-requiring process. However, we observed that the cis-SNARE complex was not properly assembled on the *ccz1*Δ and *mon1*Δ vacuoles (Fig. 3 D). We found that, in the *ccz1*Δ and *mon1*Δ strains, the syntaxin heavy chain Vam3 formed a complex only with one of the light chains, Vti1. The absence of proper cis-SNARE assembly might account for the in vitro homotypic vacuole fusion defect observed in the two mutants. Analyses of priming and docking by morphological assay suggested that the primary defect of the *ccz1*Δ and *mon1*Δ vacuoles is in the tethering/docking stage of the reaction (Fig. 4). In the priming step of homotypic fusion, Sec18-dependent hydrolysis of ATP releases Sec17 and disassembles Nyv1 and Vam7 from the cis-SNARE complex (Ungermann and Wickner, 1998; Ungermann et al., 1999). A second event may be needed to dissociate Vti1 from Vam3 (Boeddinghaus et al., 2002), or these two proteins may remain assembled. Alternatively, Vti1 might have a high affinity for Vam3 resulting in rapid reassociation with unpaired Vam3 after cis-SNARE complex dissociation. We found that Sec17 was quickly released from the *ccz1*Δ and *mon1*Δ vacuole membranes as an early event of priming (Fig. 4 B). However, we could not observe Sec17 in a complex with Vam3 in the mutant cells (Fig. 4, C and D). The binding of Sec17 to the vacuole membrane was also observed with strains lacking SNAREs (Ungermann and Wickner, 1998; Ungermann et al., 1998, 1999), suggesting that Sec17 binding and release is accomplished through the action of an as yet unidentified non-SNARE component. Thus, we suspect the Sec17 binding and release on the mutant vacuoles was accomplished through this unidentified membrane receptor(s). However, Sec17 release from the *ccz1*Δ and *mon1*Δ mutant vacuoles may not reflect a fully functional priming step.

The C-Vps/HOPS complex interacts with Ypt7 and may also function as an Ypt7 effector to achieve docking between two membranes (Sato et al., 2000; Wurmser et al., 2000). The completion of the docking stage joins the t-SNAREs, offering three "Q" α-helices, and the v-SNARE, providing one "R" α-helix based on Rothman's model, for trans-SNARE pairing. The fusion process joins the two membranes resulting in the cis-SNARE complex (Fig. 1). None of the C-Vps/HOPS complex proteins interacted with Vam3 in the *ccz1*Δ or *mon1*Δ strains, suggesting that the tethering/docking stage was impaired (Fig. 4 C). This result fits with our morphological data that indicated that the defect in the *ccz1*Δ and *mon1*Δ strains prevented the vacuoles from tethering/docking (Fig. 4 A; Table I). We found that Vps18-HA coprecipitated both Vam3 and Vti1, leading us to propose that the C-Vps/HOPS complex interacts with a Vam3-Vti1 complex rather than unpaired Vam3 (Fig. 4 C). Therefore, we propose that the Ccz1–Mon1 complex is required for regulating the SNARE complex during the coor-

dinated priming and docking stages of fusion, and particularly at the stage of tethering/docking.

The C-Vps/HOPS complex and the Ccz1–Mon1 complex are key players in the Ypt7-dependent tethering/docking stage

The C-Vps/HOPS complex is required for regulating the SNARE complex during the docking stage of fusion. The finding that the cis-SNARE complex was not properly assembled on the *ccz1*Δ and *mon1*Δ vacuoles along with the previous report revealing the association between Ccz1 and Ypt7 (Kucharczyk et al., 2001) led us to check if the Ccz1–Mon1 complex is part of the C-Vps/HOPS complex. We found that the two protein complexes colocalize, however, based on PA affinity purification they are not simply assembled into one higher order protein complex (Fig. 6 D). The Ccz1–Mon1 complex and the C-Vps/HOPS proteins appeared to interact weakly or transiently based on affinity isolation and yeast two-hybrid analyses (Fig. 6, D and E). Interestingly, the C-Vps/HOPS complex may be involved in two levels of regulation of the Ccz1–Mon1 complex; vacuolar localization of the Ccz1–Mon1 complex was lost from strains that delete one set of the C-Vps/HOPS complex (Vps11, Vps16, and Vps18), however, removing two other C-Vps/HOPS proteins (Vps39 and Vps41) in turn enriched the association of Ccz1 and Mon1 with the vacuole. Because the C-Vps/HOPS complex functions as the Ypt7 effector as well as exchange factor, it is possible that the differences in binding are due to the different Ypt7 stage that is regulated. Further data are required to resolve this speculation.

Our data and previous findings have predicted that two functionally separated complexes are required for the formation of the C-Vps complex (Wurmser et al., 2000). To further investigate C-Vps complex assembly, we checked the two-hybrid interaction of the C-Vps components in several combinations. We identified three strong two-hybrid interactions (unpublished data). In addition to the published two-hybrid interaction between binding domain (BD)-Vps11 and AD-Vps39 (Wurmser et al., 2000), we found that BD-Vps18 and AD-Vps11, and BD-Vps18 and AD-Vps39, also showed good growth on the selective plate. We then tested these three interactions in strains carrying deletions of the individual C-Vps components. We found that the interaction between BD-Vps18 and AD-Vps11 remained unaffected when other C-Vps components were deleted, indicating that the two proteins directly interact. Interestingly, the interaction between BD-Vps18 and AD-Vps39 was impaired in the *vps11*, *vps16*, and *vps33* deletion backgrounds but not in the *vps18, vps39*, and *vps41* deletion strain. This result supports the two subcomplex model for the assembly of the C-Vps complex. Specifically, Vps11, Vps16, Vps18, and Vps33 appear to be assembled first before the other subcomplex of Vps39-Vps41 can be recruited. In contrast, the interaction between BD-Vps11 and AD-Vps39 remained unaffected in the mutant backgrounds. This result supports the previously published data for a direct association between Vps11 and Vps39 that is required for C-Vps protein assembly. Together, these results suggest that after the Vps11-16-18-33 complex has formed, it recruits the Vps39-Vps41 complex through direct binding between Vps11 and Vps39 to form a C-Vps/HOPS complex.

Based on these data, we propose a model for how tethering and docking could be regulated. We suggest that the sub–C-Vps complex (Vps11, Vps16, Vps18, and Vps33) is required to recruit two complexes, one composed of Vps39-Vps41, and the other of Ccz1–Mon1. The recruitment of these two complexes appears to be two independent events, and specifically, both may not require Ypt7. It has been suggested that binding of Vps39-Vps41 to the rest of the C-Vps components is membrane dependent, although the association with the Vps39-Vps41 complex may not necessarily occur on the vacuole. However, we propose that the recruitment of the Ccz1–Mon1 complex is regulated on the vacuole membrane. Specifically, we propose that recruitment of Ccz1–Mon1 is regulated by other fusion components at a specific stage during the fusion process; one possibility is that the Ccz1–Mon1 proteins might be recruited through the C-Vps interaction with unpaired Vam3. It has been proposed by Sato et al. (2000) that the C-Vps complex functions in promoting the assembly of Vam3 into trans-SNARE complexes. In particular, they suggest that the C-Vps complex may maintain Vam3 in an unpaired stage by preventing nonproductive cis-SNARE associations. However, we found that Vam3 and Vti1 are affinity isolated together with Vps18-HA. We have demonstrated that the Ccz1–Mon1 complex is required for the interaction between the C-Vps proteins and Vam3. Accordingly, the recruitment of the Ccz1–Mon1 complex will stabilize the interaction between C-Vps and Vam3. Alternatively, the association of Vti1 with Vam3 in the *ccz1*Δ and *mon1*Δ background may reflect a nonproductive cis-SNARE association. Furthermore, it has been reported that Ccz1 preferentially binds to the nucleotide-free form of Ypt7, similar to the result seen with the two-hybrid interaction between Ypt7 and Vps39 (Wurmser et al., 2000; Kucharczyk et al., 2001). This suggests that the Ccz1–Mon1 complex may interact with Ypt7 and bring Ypt7 to its guanine nucleotide exchange factor, Vps39. It is still not known, however, if the Ccz1–Mon1 complex is required as part of the Ypt7 GDP/GTP cycle. Overexpression of Ypt7 or expression of an Ypt7 mutant that cannot bind nucleotide suppresses the Ccz1 deletion phenotype (Kucharczyk et al., 2001). However, the Ccz1–Mon1 complex might have another role after GDP/GTP exchange. Expression of $Ypt7^{Q68L}$, a mutant form of Ypt7 that remains in the GTP-bound state and that has a wild-type vacuole phenotype, could not prevent vacuole fragmentation in strains deleted for *CCZ1* or *MON1* (unpublished data). Hence, we suggest that the Ccz1–Mon1 complex may function in part as the Ypt7 downstream effector during the tethering/docking stage. Our data suggest that the Ccz1–Mon1 complex is down-regulated from the vacuole by Vps39-Vps41. The particular timing that is needed for this down-regulation may require activation of the Vps39-Vps41 complex. It is possible that down-regulation occurs before or during trans-SNARE pairing, although further data are required to carefully dissect this part of the fusion process.

Overall, we propose that the Ccz1–Mon1 complex is required for regulating the SNARE complex during the coordinated priming and docking stages of fusion, and particu-

larly at the stage of tethering/docking. Accordingly, the absence of Ccz1 or Mon1 prevents subsequent fusion. Further studies of the C-Vps/HOPS proteins and their interaction with the Ccz1–Mon1 complex and Ypt7 and with SNARE proteins will be necessary to understand how the priming and docking steps are regulated to achieve functional SNARE association.

Materials and methods

Strains, media, reagents, and antisera/antibodies

The yeast strains used in this study are listed in Table II. Media for growth of yeast strains and reagents were described previously (Wang et al., 2001a). FM 4-64 dye was obtained from Molecular Probes. Antisera against Mon1 and Pep4 were described previously (Wang et al., 2002a). Antisera against Ypt7, Sec17, Sec18, Nyv1, Vti1, Vam7, and Vam3 were provided by Dr. William Wickner (Dartmouth Medical School, Hanover, NH). Yeast two-hybrid plasmid of Vps11, Vps16, Vps18, and Vps39 and pPA-Vps16 were provided by Dr. Scott Emr (University of California, San Diego, CA). Antibody against Pho8 was obtained from Molecular Probes, and the anti-HA antiserum was purchased from Santa Cruz Biotech, Inc. To prepare antiserum against Ccz1, the sequence encoding the NH_2 terminus of Ccz1 (359–965 bp) was PCR amplified and fused to the COOH terminus of GST. The resulting plasmid was transformed into *E. coli* strain BL21. Fusion proteins were induced by adding isopropyl-1-thio-β-D-galactopyranoside (IPTG) followed by column purification to generate antigen. Polyclonal rabbit antiserum was produced using standard procedures as described previously (Wang et al., 2001a).

Disruption, epitope tagging, gene cloning, and plasmid construction

A PCR-based, one-step procedure was used to tag chromosomal genes with a sequence encoding PA or GFP and its derivatives (Reggiori et al., 2003). To construct a fusion of PA with Ccz1, PA-CCZ1, the *CCZ1* ORF was PCR amplified using pCCZ1(416) as a template. The resulting PCR products were fused with pCuPrA(416) (Kim et al., 2002) to generate pCuPA-CCZ1(416). The plasmid PA-Vps16(416) was described previously (Sato et al., 2000). All oligonucleotide sequences and additional details of the plasmid constructions will be provided upon request. To construct the two-hybrid plasmid of Vps33 and Vps41, the corresponding ORFs were PCR amplified from a wild-type genome. The resulting PCR products were digested and fused with pGAD (James et al., 1996). To construct the bait plasmid of Mon1, the corresponding ORFs were PCR amplified from a wild-type genome. The resulting PCR products were digested and fused with pGBDU (James et al., 1996).

Vacuole preparation and in vitro vacuole fusion assay

Preparation of cytosol and vacuoles was described previously (Haas, 1995). To compare the in vitro fusion activity, vacuoles were prepared separately from the *pep4*Δ and *pho8*Δ backgrounds. The standard 30-μl reaction contained 3-μg vacuoles prepared from the *pep4*Δ (BJ3505) and *pho8*Δ (DKY6281) strains in physiological salts (Haas, 1995). To examine deletion strain vacuole fusion, every set of experiments was assayed with

Table II. ***S. cerevisiae*** **strains used in this study**

Strain	Genotype	Reference
SEY6210	*MATα leu2-3112 ura3-52 his3Δ-200 trp1Δ-901 lys2-801 suc2Δ-9 GAL*	Robinson et al., 1988
BJ3505	*MATα pep4::HIS3 prb1-Δ*1.6R *HIS3 lys2-208 trp1Δ-101 ura3-52 gal2 can*	Haas, 1995
BY4742	*MATα leu2Δ ura3Δ his3Δ lys2Δ*	ResGen
CWY3	SEY6210 *ccz1Δ::HIS5 S.p.*	Wang et al., 2002a
CWY14	SEY6210 *mon1Δ::HIS5 S.p. pho8Δ::TRP1*	This study
CWY15	SEY6210 *ccz1Δ::HIS5 S.p. pho8Δ::TRP1*	This study
CWY23	SEY6210 *ypt7Δ::HIS3 pep4Δ::URA3*	This study
CWY33	BJ3505 *mon1Δ::TRP1*	This study
CWY34	BJ3505 *ccz1Δ::TRP1*	This study
CWY42	BJ3505 *VPS18-HA::TRP1*	This study
CWY47	CWY33 *VPS18-HA::KanMX*	This study
CWY57	CWY34 *VPS18-HA::KanMX*	This study
CWY173	SEY6210 *Vps18-HA::HIS3 S.k. Vps39-HA::Trp*	This study
DKY6281	SEY6210 *pho8Δ::TRP1*	Haas, 1995
JSY1	SEY6210 *mon1Δ::HIS5 S.p.*	Wang et al., 2002a
K91-1A	*MATα ura3 pho8::pAL134 pho13::pH13 lys1*	Haas, 1995
*pbi2*Δ	BY4742 *pbi2Δ::KanMX*	ResGen
PJ69-4A	*MATα trp1-901 leu2-3,112 ura3-52 his3-200 gal4Δ gal80Δ LYS2::GAL1-HIS3 GAL2-ADE2 met2::GAL7-lacZ*	James et al., 1996
PSY32	SEY6210 *VPS33-HA::HIS3 S.k.*	This study
PSY33	SEY6210 *VPS39-HA::HIS3 S.k.*	This study
PSY43	SEY6210 *CCZ1-YFP::HIS3 S.k. VPS18-CFP::KanMX*	This study
PSY46	SEY6210 *CCZ1-GFP::HIS3*	Wang et al., 2002a
PSY101	SEY6210 *CVT9-GFP::HIS3 S.k.*	This study
PSY156	DKY6281 *Mon1-PA::KanMX*	This study
PSY157	DKY6281 *Ccz1-PA::KanMX*	This study
PSY288	BJ3505 *Ccz1-PA::TRP1*	This study
PSY287	BJ3505 *Mon1-PA::TRP1*	This study
*vam7*Δ	BY4742 *vam7Δ::KanMX*	ResGen
*vps11*Δ	BY4742 *vps11Δ::KanMX*	ResGen
*vps16*Δ	BY4742 *vps16Δ::KanMX*	ResGen
*vps18*Δ	BY4742 *vps18Δ::KanMX*	ResGen
*vps39*Δ	BY4742 *vps39Δ::KanMX*	ResGen
*vps41*Δ	BY4742 *vps41Δ::KanMX*	ResGen

duplicate samples, and the data from three independent experiments were averaged. To examine PA-Ccz1 and/or PA-Mon1 vacuole fusion activity, every set of experiments was assayed and averaged from six independent experiments with or without the addition of 0.5 μl of antiserum against Atg2. To examine Sec17 release, 90-μl standard reactions without the addition of cytosol were aliquoted for each time point. Reactions were stopped by transferring to ice for 1–2 min and spun at 10,000 *g* for 4 min. Supernatant and pellet fractions were TCA precipitated separately followed by Western blot analysis. A similar approach was used for examining release of Mon1. The microscopy docking/fusion assay was performed as described (Wang et al., 2001b).

OptiPrep™ density gradient and sucrose velocity gradient analyses

To examine the localization of Ccz1–Mon1 and the C-Vps complex, we performed OptiPrep™ density gradient analysis using a modification of a previously described procedure (Wang et al., 2002a). The gradient was 10–55% OptiPrep™ and centrifugation was performed for 12 h.

To examine the vacuolar SNARE complex, we performed sucrose gradient analysis. Purified vacuoles (0.5 mg) were pelleted and resuspended in 300-μl PS200 buffer containing 1% Triton X-100. Vacuoles were solubilized on ice for 20 min and loaded on the top of a 12-ml 10–60% linear sucrose gradient (PS200). The gradient was centrifuged at 4°C for 14 h. A total of 13 fractions were collected from the top of the gradient and TCA precipitated followed by Western blot analysis.

Immunoprecipitation and PA affinity purification

To analyze the association with the C-Vps and SNARE complexes, a 750-μl standard fusion reaction was set up in the presence of an ATP regeneration system (ARS; +ATP) or the absence of ARS with the addition of 30 U/ml apyrase (−ATP). All reactions were incubated at 27°C for 15 min and chilled on ice for 2 min. Vacuoles were reisolated by spinning at 10,000 *g* for 5 min, followed by coimmunoprecipitation as described (Wang et al., 2002a). The protocol for coimmunoprecipitation with Vps18-HA and Vam3 was as described previously (Wang et al., 2002a). The PA affinity purification procedure using IgG sepharose was modified from Sato et al. (2000). Spheroplasts were osmotically lysed on ice in lysis buffer (50 mM Tris, pH 7.5, 150 mM NaCl, 2 mM EDTA, 0.5% Triton X-100, 1× complete protease inhibitors (Roche Molecular Biochemicals), and 1 mM PMSF). After 20 min solubilization on ice, total cell lysates were centrifuged at 10,000 rpm for 5 min at 4°C. To the resulting supernatant, 25 μl of IgG-Sepharose 6 Fast Flow was added and incubated at 4°C for 2 h. Sepharose beads were washed eight times with lysis buffer. Bound proteins were eluted in MURB (Wang et al., 2002a), followed by SDS-PAGE and Western blot analysis.

Microscopy

All strains used for microscopy were grown in synthetic minimal medium with dextrose (SMD) to mid-log phase. In vivo FM 4-64 staining and microscopy analyses were performed as described previously (Wang et al., 2002a).

We thank Drs. William Wickner and Scott Emr for supplying antiserum and plasmids. We thank members of the Klionsky laboratory for helpful discussions.

This work was supported by Public Health Service grants GM53396 and GM50403 from the National Institutes of Health to D.J. Klionsky and L.S. Weisman, respectively.

Submitted: 13 August 2003
Accepted: 23 October 2003

References

Boeddinghaus, C., A.J. Merz, R. Laage, and C. Ungermann. 2002. A cycle of Vam7p release from and PtdIns 3-P-dependent rebinding to the yeast vacuole is required for homotypic vacuole fusion. *J. Cell Biol.* 157:79–89.

Fasshauer, D., D. Bruns, B. Shen, R. Jahn, and A.T. Brunger. 1997. A structural change occurs upon binding of syntaxin to SNAP-25. *J. Biol. Chem.* 272: 4582–4590.

Haas, A. 1995. A quantitative assay to measure homotypic vacuole fusion in vitro. *Methods Cell Sci.* 17:283–294.

James, P., J. Halladay, and E.A. Craig. 1996. Genomic libraries and a host strain designed for highly efficient two-hybrid selection in yeast. *Genetics.* 144: 1425–1436.

Kato, M., and W. Wickner. 2003. Vam10p defines a Sec18p-independent step of priming that allows yeast vacuole tethering. *Proc. Natl. Acad. Sci. USA.* 100: 6398–6403.

Kim, J., Y. Kamada, P.E. Stromhaug, J. Guan, A. Hefner-Gravink, M. Baba, S. Scott, Y. Ohsumi, W.A. Dunn, Jr., and D.J. Klionsky. 2001. Cvt9/Gsa9 functions in sequestering selective cytosolic cargo destined for the vacuole. *J. Cell Biol.* 153:381–396.

Kim, J., W.-P. Huang, P.E. Stromhaug, and D.J. Klionsky. 2002. Convergence of multiple autophagy and cytoplasm to vacuole targeting components to a perivacuolar membrane compartment prior to de novo vesicle formation. *J. Biol. Chem.* 277:763–773.

Kucharczyk, R., S. Dupre, S. Avaro, R. Haguenauer-Tsapis, P.P. Slonimski, and J. Rytka. 2000. The novel protein Ccz1p required for vacuolar assembly in *Saccharomyces cerevisiae* functions in the same transport pathway as Ypt7p. *J. Cell Sci.* 113:4301–4311.

Kucharczyk, R., A.M. Kierzek, P.P. Slonimski, and J. Rytka. 2001. The Ccz1 protein interacts with Ypt7 GTPase during fusion of multiple transport intermediates with the vacuole in *S. cerevisiae*. *J. Cell Sci.* 114:3137–3145.

Mayer, A., W. Wickner, and A. Haas. 1996. Sec18p (NSF)-driven release of Sec17p (α-SNAP) can precede docking and fusion of yeast vacuoles. *Cell.* 85:83–94.

McNew, J.A., F. Parlati, R. Fukuda, R.J. Johnston, K. Paz, F. Paumet, T.H. Sollner, and J.E. Rothman. 2000. Compartmental specificity of cellular membrane fusion encoded in SNARE proteins. *Nature.* 407:153–159.

Reggiori, F., C.W. Wang, P.E. Stromhaug, T. Shintani, and D.J. Klionsky. 2003. Vps51 is part of the yeast Vps fifty-three tethering complex essential for retrograde traffic from the early endosome and the Cvt vesicle completion. *J. Biol. Chem.* 278:5009–5020.

Robinson, J.S., D.J. Klionsky, L.M. Banta, and S.D. Emr. 1988. Protein sorting in *Saccharomyces cerevisiae*: isolation of mutants defective in the delivery and processing of multiple vacualor hydrolases. *Mol. Cell Biol.* 8:4936–4958.

Sato, T.K., P. Rehling, M.R. Peterson, and S.D. Emr. 2000. Class C Vps protein complex regulates vacuolar SNARE pairing and is required for vesicle docking/fusion. *Mol. Cell.* 6:661–671.

Stromhaug, P.E., and D.J. Klionsky. 2004. Cytoplasm to vacuole targeting. In: D.J. Klionsky (ed). Autophagy. Landes Bioscience: Georgetown, TX, in press.

Ungermann, C., B.J. Nichols, H.R.B. Pelham, and W. Wickner. 1998. A vacuolar v-t-SNARE complex, the predominant form in vivo and on isolated vacuoles, is disassembled and activated for docking and fusion. *J. Cell Biol.* 140: 61–69.

Ungermann, C., G.F. von Mollard, O.N. Jensen, N. Margolis, T.H. Stevens, and W. Wickner. 1999. Three v-SNAREs and two t-SNAREs, present in a pentameric *cis*-SNARE complex on isolated vacuoles, are essential for homotypic fusion. *J. Cell Biol.* 145:1435–1442.

Ungermann, C., and W. Wickner. 1998. Vam7p, a vacuolar SNAP-25 homolog, is required for SNARE complex integrity and vacuole docking and fusion. *EMBO J.* 17:3269–3276.

Wang, C.-W., J. Kim, W.-P. Huang, H. Abeliovich, P.E. Stromhaug, W.A. Dunn, Jr., and D.J. Klionsky. 2001a. Apg2 is a novel protein required for the cytoplasm to vacuole targeting, autophagy, and pexophagy pathways. *J. Biol. Chem.* 276:30442–30451.

Wang, Y.E., E.J. Kauffman, J.E. Duex, and L.S. Weisman. 2001b. Fusion of docked membranes requires the armadillo repeat protein Vac8p. *J. Biol Chem.* 276:35133–35140.

Wang, C.-W., P.E. Stromhaug, J. Shima, and D.J. Klionsky. 2002a. The Ccz1-Mon1 protein complex is required for the late step of multiple vacuole delivery pathways. *J. Biol. Chem.* 277:47917–47927.

Wang, L., E.S. Seeley, W. Wickner, and A.J. Merz. 2002b. Vacuole fusion at a ring of vertex docking sites leaves membrane fragments within the organelle. *Cell.* 108:357–369.

Wickner, W. 2002. Yeast vacuoles and membrane fusion pathways. *EMBO J.* 21: 1241–1247.

Wickner, W., and A. Haas. 2000. Yeast homotypic vacuole fusion: A window on organelle trafficking mechanisms. *Annu. Rev. Biochem.* 69:247–275.

Wurmser, A.E., T.K. Sato, and S.D. Emr. 2000. New component of the vacuolar class C-Vps complex couples nucleotide exchange on the Ypt7 GTPase to SNARE-dependent docking and fusion. *J. Cell Biol.* 151:551–562.